Sirtuin 1 deficiency decreases bone mass and increases bone marrow adiposity in a mouse model of chronic energy deficiency

Loïc Louvet, Damien Leterme, Séverine Delplace, Flore Miellot, Pierre Marchandise, Véronique Gauthier, Pierre Hardouin, Christophe Chauveau, Olfa Ghali Mhenni

Sirtuin 1 deficiency decreases bone mass and increases bone marrow adiposity in a mouse model of chronic energy deficiency

Loïc Louvet, Damien Leterme, Séverine Delplace, Flore Miellot, Pierre Marchandise, Véronique Gauthier, Pierre Hardouin, Christophe Chauveau*and Olfa Ghali Mhenni*

***Same authorship. Correspondence: olfa.ghali@univ-littoral.fr**

Physiopathologie des Maladies Osseuses Inflammatoires (PMOI) EA4490, Univ. Littoral Côte d'Opale F-62200 Boulogne-sur-Mer, Univ. Lille F-59000 Lille, CHU Lille F-59000 Lille, France.

1. Introduction

High bone marrow adiposity (BMA, defined as the proportion of the BM cavity volume occupied by adipocytes) is frequently associated with osteoporosis or compromised bone quality, and it is the result of mechanical unloading [1], ageing [2,3], menopause [3], diabetes [4,5] and obesity [6,7]. Surprisingly, this association was also found in anorexia nervosa (AN) patients [8]. Indeed, histological and magnetic resonance imaging (MRI) analyses demonstrated an increase in BMA in patients with osteoporosis [9-12]. More recently, a negative correlation was shown between the fraction of fat in the bone marrow cavity and the bone mineral density (BMD) at the femoral neck and at the hip of anorexic patients in multiple anatomical subregions, even after weight recovery [13].

It is also well known that BMA increases with age in a bone-site specific manner [14-17] and is generally linked to poor bone quality [18-20]. Marrow adipose tissue (MAT) is a repository for storing excess energy and it protects bone from free fatty acids that can negatively impact osteoblastogenesis through lipotoxicity [21,22], but the origin and function of MAT are complex and remain incompletely understood.

Marrow adipocytes originate from skeletal stem cells (SSCs), which is also where bone-forming osteoblasts come from [23-25]. Moreover, it has been demonstrated that the accumulation of marrow adipocytes observed in bone loss is caused by a shift in the commitment of SSCs from the osteogenic pathway to the adipogenic pathway [26]. This suggested the existence of a competitive relationship between these two pathways. Moreover, bone marrow stromal cells (BMSCs) from aged mice express more adipocytic transcripts and fewer osteoblastic transcripts than what is observed in BMSCs from young animals [27].

A variety of endogenous modulators of signalling pathways, including Wnts [28], bone morphogenetic proteins [29] and glucocorticoids [30,31] can influence this process towards one direction or the other. Moreover, the histone deacetylase (HDAC) family was also shown to influence the fate of differentiating mesenchymal progenitor cells by removing acetyl groups from lysine residues in histones and other proteins, thus altering chromatin structure and gene expression [32,33]. It has been reported that HDAC3 is required for the maintenance of bone mass during ageing [34,35]. In contrast, HDAC1 and HDAC2 are required for adipocyte differentiation because genetic deletion of both HDAC1 and HDAC2 robustly blocks the effects of pro-adipogenic stimuli [36].

In addition to its effects on the regulation of life span in mammals and protection against age-associated diseases such as obesity, diabetes [37], and Alzheimer's disease [38],

Sirt1 is a class III HDAC that can also regulate cell differentiation of SSCs into osteoblasts and adipocytes. Indeed, *in vivo*, activation of Sirt1 restores bone mass, structure, and biomechanical properties in ovariectomized female mice [39], and it protects against age-associated bone loss in male mice [40]. Moreover, Sirt1 promotes cortical bone formation [41], and adult Sirt1 haplo-insufficient female mice display low bone mass characterized by reduced bone formation [42]. In vitro studies demonstrated that activation of Sirt1 promotes osteoblastic differentiation at the expense of adipogenesis [43-46]. Sirt1 is known to be present in both the cytosol and the nucleus, which is where it deacetylates histones and a host of nonhistone-regulatory proteins such as p53, peroxisomal proliferator-activated receptor-γ coactivator-1α (PGC-1α), runt-related transcription factor 2 (Runx2), Forkhead box protein O (Foxo), and nuclear factor-κB (NF κB) [47].

Activation of Sirt1 by treating BMSCs with resveratrol induces their differentiation into osteoblasts [45,46,48,49]. A decrease in Sirt1 expression caused by sirtinol treatment promotes adipocytic differentiation [50,51]. Importantly, caloric restriction has been shown to stimulate the expression and activity of Sirt1 in various mammalian tissues, such as liver and white adipose tissue [52,53], but it has also been shown that caloric restriction induces a decrease in the level of Sirt1 mRNA in the cerebellum and midbrain [54]. However, at present, no study has focused on the regulation of Sirt1 in bone marrow. Further, no study has focused on the link between Sirt1, BMA and osteoporosis related to AN. Thus, the aims of this work were to (i) determine BMA and bone changes in a mouse model replicating the phenotypes of anorexia nervosa [55]; (ii) determine the expression of Sirt1 in BMSCs extracted from these mice and identify their differentiation capacities; (iii) study the effects of pharmacological activation and inhibition of Sirt1 on the osteoblastogenesis and adipogenesis of these cells; and (iiii) delineate the molecular mechanism by which Sirt1 could regulate osteogenesis in an SBA model.

2. Materials and methods

2.1. Animals

To generate a separation-based anorexia (SBA) model, the following steps were performed: Seven-week-old female C57BL/6J mice were purchased from Charles River Laboratories (St Germain sur l'Abresle, France). This strain was chosen because of its use in numerous studies related to bone alterations associated with calorie restriction, and because it displays a medium level of BMA which allows to detect an increase as well as a decrease.

Mice were housed 6 per cage in a controlled room temperature (22°C+/- 1°C) under a 12-hour dark/light cycle (lights off at 10 a.m.), and the mice had free access to water. Mice were acclimatized one week before the start of the protocol. The SBA model was generated as previously described [55]; eight weeks of SBA protocol to induce a moderate body weight loss of 18.17% relative to day D0 and 33.24% relative to control (CT) mice. Indeed, the SBA group was fed daily with an access to food gradually reduced from 6 h to 2 h a day along the protocol. The SBA mice were gathered together in regular cages for the periods of feeding. The CT group was housed in standard conditions, in collective cages, with water and food ad libitum. This study was specifically approved by the Committee on the Ethics of Animal Experiments (CEEA) of Nord-Pas de Calais, France (permit number: CEEA#2016070717275082).

Seven-week-old female floxed mice (C57BL6, 129-sirt1<tm1Ygu</J-SN 8041) and their wild type counterparts (C57BL6, 129SF2/J-SN101045) were purchased from the Jackson Laboratory and delivered to our laboratory by Charles River Laboratories. Animals were housed under specific pathogen-free conditions with free access to water and food. They were sacrificed at the age of sixteen weeks.

2.2. Dual energy X-ray absorptiometry (DEXA) analysis

Bone mineral content (BMC), lean mass and fat mass were analysed by using the Lunar PIXImus Mouse Densitometer (GE Healthcare, Madison, WI) as previously described [55].

2.3. Primary bone marrow cell cultures

Primary bone marrow-derived cells were harvested from the tibias and femurs of CT and SBA mice and differentiated into both osteoblasts and adipocytes, as described in our previous work [31]. After reaching confluence in culture, BMSCs were treated for two weeks with 10µM of sirtinol and 10µM of resveratrol (Santa Cruz Biotechnology, Santa Cruz, CA, USA). The medium containing different treatments was replaced every three days during all periods of co-differentiation.

2.4. Organotypic cultures

Bones for organotypic cultures like the other ones were collected at the end of the eight-weeks protocol, so when mice were sixteen-week-old. Tibias from CT and SBA mice were removed and cleaned of connective tissue. The ends were carefully cut to preserve the bone marrow, and the tibias were treated for 10 days with 100µM of resveratrol in a standard

medium containing alpha Minimum Essential Medium (α-MEM) (PAN Biotech, Dutsher, Brumath, France) supplemented with 10% foetal calf serum (FCS) (PAN Biotech), 2 mM glutamine (PAN Biotech), 50 IU/ml penicillin (PAN Biotech), and 50 µg/ml streptomycin (PAN Biotech). The medium was replaced every three days.

2.5. RNA extraction, reverse transcription and real-time PCR

Total RNA from BMSC cultures was extracted as previously described [31].

For organotypic culture, each tibia was crushed in a mortar and pestle in liquid nitrogen. The powder obtained from each tibia was dissolved in 5 ml of Extract-all (Eurobio, Les Ulis, France) and 1 ml of RNA later (Sigma Aldrich, France). One millilitre of this suspension was added to 0,2 ml of chloroform (Sigma Aldrich), and the mix was transferred to 2 ml Maxtract High Density tubes (Qiagen) and centrifuged at 4°C at 15000 g for 15 minutes. The aqueous phase was transferred to a column from a RNeasy Micro Kit (Qiagen), and RNA extraction was performed according to the manufacturer's instructions.

Reverse transcription and real-time PCR were performed as previously described [56]. The sequences of the primers (TibMolBiol, Berlin, Germany) for each of the analysed genes are shown in Table 1.

Table 1
Primers sequences and conditions of PCR.

Gene	Primer Sequences	Annealing temperature	Product length	GenBank
Runx2	F: GCCGGGAATGATGAGAACTA R: GGACCGTCCACTGTCACTTT	62°C	200 bp	NM_001146038.2
OC	F: AAGCAGGAGGGCAATAAGGT R: CGTTTGTAGGCGGTCTTCA	60°C	364 bp	NM_007541.3
OSX	F: CTAGTTCCTATGCTCCGACC R: TCATCACATCATCATCGTG	54°C	237 bp	NM_130458.1
ALP	F: CAAAGGCTTCTTCTTGCTGGT R: AAGGGCTTCTTGTCCGTGTC	60°C	257 bp	NM_007431.3
PPARγ -2	F: GGTGAAACTCTGGGAGATTCT R: CAACCATTGGGTCAGCTCTTG	55°C	268 bp	NM_011146.3
Leptin	F: CTCATGCCAGCACTCAAAAA R: AGCACCACAAAACCTGATCC	62°C	197 bp	NM_008493.3
Glut4	F: ACTCTTGCCACACAGGCTCT R: AATGGAGACTGATGCGCTCT	62°C	174 bp	NM_009204.2
Adiponectin	F: CCCAGTCATGCCGAAGA R: TACATTGGGAACAGTGACGC	62°C	354 bp	NM_009605.4
GAPDH	F: GGCATTGCTCTCAATGACAA R: TGTGAGGGAGATGCTCAGTG	62°C	200 bp	NM_008084.1
18S	F: ATTCCGATAACGAACGAGAC	60°C	297 bp	NR_003278.3

	R: GCTTATGACCCGCACTTACT			
Sirt1	F: TAGGGAACCTTTGCCTCATC R: GGCATATTCACCACCTAGCC	51°C	100 bp	NM_019812.2
Fasn	F: CTGCCCAGCCCATAAGAGTT R: CGTCTCCACTCCCGAATGT	59°C	162 bp	NM_007988.3
Plin1	F: CACCATCTCTACCCGCCTTC R: GGGTGTTGGCGGCATATT C	58°C	149 bp	NM_001113471.1
Cidec	F: GGCAGTGAGCACGGCAGT R: ATGATGCCTTTGCGAACCTT	58°C	117 bp	NM_001301295.1

2.6. Western blot analysis and immunoprecipitation

Western blot analysis was performed as previously described [56]. For this study, rabbit polyclonal antibodies (Sirt1, Runx2, and Foxo1) and a mouse monoclonal antibody (β-actin) were used (Santa Cruz Biotechnology). Runx2 lysine acetylation and Foxo1 lysine acetylation were analysed by immunoprecipitation using an anti-acetyl-lysine antibody (Santa Cruz Biotechnology).

2.7. Mineralization staining and quantification

Mineralization was studied by staining with alizarin red, and it was quantified according the protocol previously described [31].

2.8. µCT analysis

Tibias from CT and SBA were scanned using a Skyscan 1172 microCT device (Bruker MicroCT, kontich, Belgium). The software suite provided by the manufacturer was used for image acquisition, reconstruction, analysis and 3D visualisation (Skyscan 1172©,NRecon©,Dataviewer, CTAn©, CTVox^{TM}). Analysis of tibia trabecular bone volume/tissue volume (BV/TV) ratio, cortical thickness (Ct.Th), trabecular thickness (Tb.Th), trabecular number (Tb.N) and trabecular space (Tb.Sp) of all animals were determined as previously described [57].

2.9. Bone marrow adipocyte density

Tibias from CT and SBA animals were fixed in cold 10% neutral buffered formalin for 24 hours. These undecalcified tibias were dehydrated, methylmethacrylate-embedded, and sectioned at a thickness of 6 µm per slice with a microtome (RM2255, Leica Biosystems). The sections were placed on gelatine-coated slides, deplasticized and stained with toluidine blue (Fisher Chemical, France). Adipocytes at proximal tibias were measured in an area from 200 to 1000 microns below the growth plate. Image acquisition was performed on an

Axiokop40 microscope (Zeiss, Germany) using Histolab and Archimed software (Excilone). The number of adipocytes per marrow area (N. Ad/Ma.Ar) (cells/mm^2) was measured by tracing adipocytes with ImageJ software (NIH).

2.10. Statistical analysis

All cell culture experiments were performed in triplicate and repeated four times. The number of tibias used in this study varied between 4 and 18 (see details below each figure). The mean value and S.E.M. (Standard Error of the Mean) was calculated for the groups. Mann-Whitney's test for statistical significance was performed by using GraphPad Prism software. Differences with $p < 0.05$ were considered statistically significant.

3. Results and Discussion

3.1. Separation-based anorexia induces an alteration of bone architecture and an increase in BMA

The aim of this study was to determine the consequences of a long-term energy deficit on bone architecture and BMA and then to identify the mechanisms regulating BMA in this context. Thus, a mouse model recapitulating the consequences of AN was used; the mice were exposed to a separation-induced increase in energy expenditure and a time-restricted feeding that prevented compensatory feeding (separation-based anorexia, SBA) [55]. This protocol rapidly induced a body weight loss of approximately 18% relative to mice at day zero of the protocol ($p<0.05$) and approximately 33% relative to control (CT) mice at the endpoint ($p<0.05$) (Fig. 1). This was associated with a significantly low fat mass (-55% vs CT mice), a low lean mass (- 21% vs CT mice), a low total body bone mineral content (BMC) (-14% vs CT mice), a low femur BMC (-28.5%) and a low lumbar spine BMC (-8.5%). Trabecular and cortical bone architecture was also significantly altered. Indeed, the SBA protocol induced lower cortical thickness (Ct.Th) (-17%), a lower tibia trabecular bone volume/tissue volume ratio (BV/TV) (-14%) and lower trabecular thickness (Tb.Th) (-12%) (Fig. 2A-C). However, the SBA protocol did not induce a significant difference in the trabecular number (Tb. N) or in the trabecular space (Tb.Sp) (Fig. 2D, E). Interestingly, SBA mice presented high BMA at the proximal tibia (a two-fold increase compared to CT mice) (Fig. 2F). Some studies demonstrated an increase in BMA associated with bone alteration in anorexic patients [9-10,13]. In rodent models of food or calorie restriction, some published studies focused on BMA. Indeed, it is demonstrated that 9 weeks of a 30% restriction on food on 3-week-old

male mice induced low BV/TV (-11%), Ct.Th (-27%), and body weight (-40%) and high BMA (700%) compared to CT mice [58]. More recently, it has been shown that 6 weeks of a 30% calorie-restricted diet on 9-week-old female mice induced an increase in tibia BMA of 700% compared to the *ad libitum* group [59]. Interestingly, in these two studies, the very high increase in BMA is associated with a body weight increase of 80% vs day 0 of the experiment [58] or an endpoint body weight similar to that of day 0 of the experiment [59]. In contrast, a calorie restriction protocol (low carbohydrate feeding) for 12 weeks on 6-month-old Sprague-Dawley female rats demonstrated that restricted rats displayed body weight loss (20% vs day 0 and 25% vs CT rats), a low volumetric BMD at the proximal tibia (-14%) and only a two-fold increase in BMA measured at the distal femur [60]. In contrast to these studies, 10 weeks of caloric restriction in 14-week-old male mice led to a body weight loss of 30% (relative to CT mice) and a total disappearance of BM adipocytes in the distal femur [61]. Thus, the SBA protocol used for the present study seems to be close to that of Baek et al [60], considering that the SBA mice in this study display (i) a level of food intake similar to CT mice but with a high level of energy expenditure, (ii) a body weight decrease of approximately 20% vs their body weight at day 0 of the experiment, and (iii) a two-fold increase in BM adipocyte density. Moreover, these data suggest that restriction-induced changes in BMA and bone quality may be modulated by age, sex, severity and duration of the restriction.

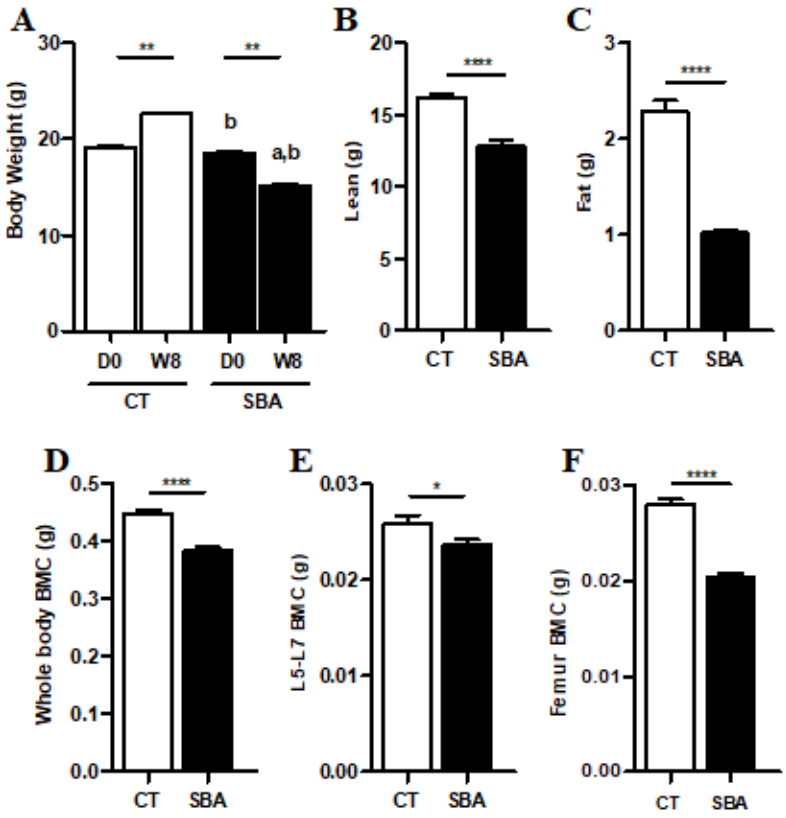

Fig. 1. Effects of SBA protocol on body weight and composition.

Measures were performed on control (CT) and separated-based anorexia (SBA) mice. A: body at the beginning (D0) and after 8 weeks of SBA protocol (8W). Whole body lean mass (B), fat mass (C), bone mineral content (BMC) (D). BMC of lumbar vertebrae 5 to 7 (E) and of femur (F) were analysed by Dexa. Results are mean +/- SEM representative of three independent experiments; n=6/group. $^{*}p<0.05$. $^{**}p<0.005$. $^{****}p<0.0001$.

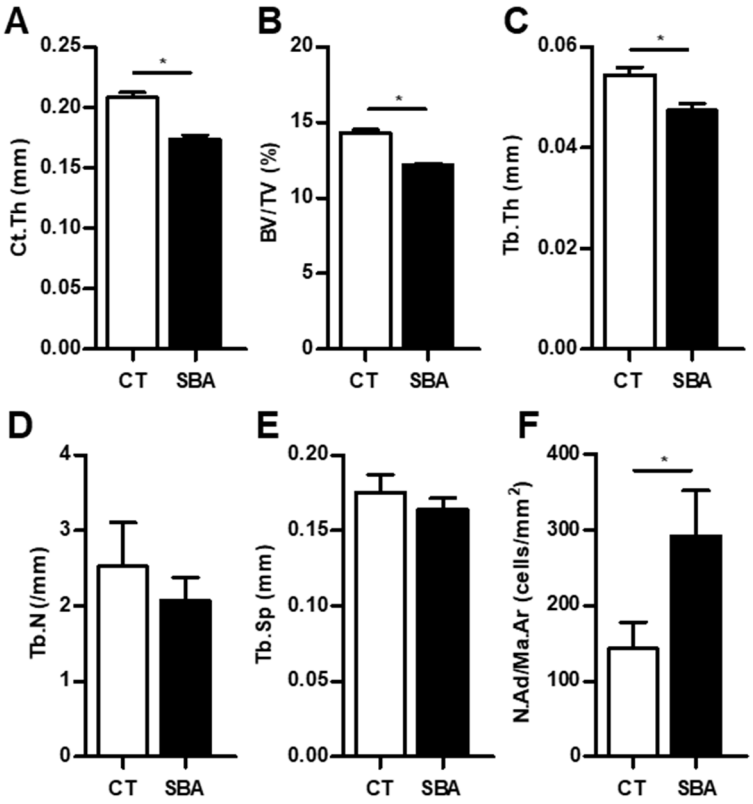

Fig. 2. Effects of SBA protocol on bone microarchitecture and bone marrow adipocyte density.

Cortical thickness (Ct.Th) (A), trabecular bone volume/tissue volume (BV/TV) ratio (B), trabecular thickness (Tb.Th) (C), trabecular number (Tb.N) (D) and trabecular space (Tb.Sp) (E) were assessed by micro-CT of tibias of CT and SBA mice. Number of adipocytes per marrow area (N.Ad/Ma.Ar) (F) was determined by histological analysis of tibias of CT and SBA mice. 6 tibias in each group were analysed. Results are mean +/- SEM; n=6/group. $^{*}p<0.05$ vs. CT mice.

3.2. Separation-based anorexia induces an imbalance between osteoblastogenesis and adipogenesis

Osteoblasts and adipocytes are derived from a common mesenchymal progenitor [62,63]. Thus, to determine the mechanisms driving the increase in BMA associated with bone loss in SBA mice, we tested the hypothesis that BMSCs from SBA mice preferentially differentiated down the adipogenic pathway. Interestingly, in the co-differentiation medium that allows both adipogenesis and osteogenesis [31], BMSCs from SBA mice displayed very fast adipogenesis compared to BMSCs from CT mice. Indeed, their lipid droplets appeared

after 3 days of induction in codifferentiation medium, while it took 10 days for BMSCs from CT mice to exhibit those effects (Fig. 3A). This fast adipogenesis was associated with high mRNA levels of adipocytic markers, which were measured at 14 days of codifferentiation; the experimental group had higher levels of each of the measured genes than the BMSCs from CT mice at the same time (*PPARγ* +37%, *adiponectin* +505%, *leptin* +610% and *Glut4* +243%) (Fig. 3C-F), and they exhibited an increase in genes related to lipid storage, such as fatty acid synthase (*Fasn*) (+145%), *perilipin 1* (*Plin1*) (+231%) and cell-death inducing *DFFA-like effector c* (*Cidec*) (+725%) (Fig. 3G-I). Interestingly, after just 48 hours of adhesion in a standard proliferative medium, the native unstimulated BMSCs from SBA mice already presented high levels of *PPAR-γ* mRNA (+47% vs CT) (Fig. 3B). This culture duration was chosen because of its brevity, which allowed minimizing the time for cells to change after leaving the in vivo state.

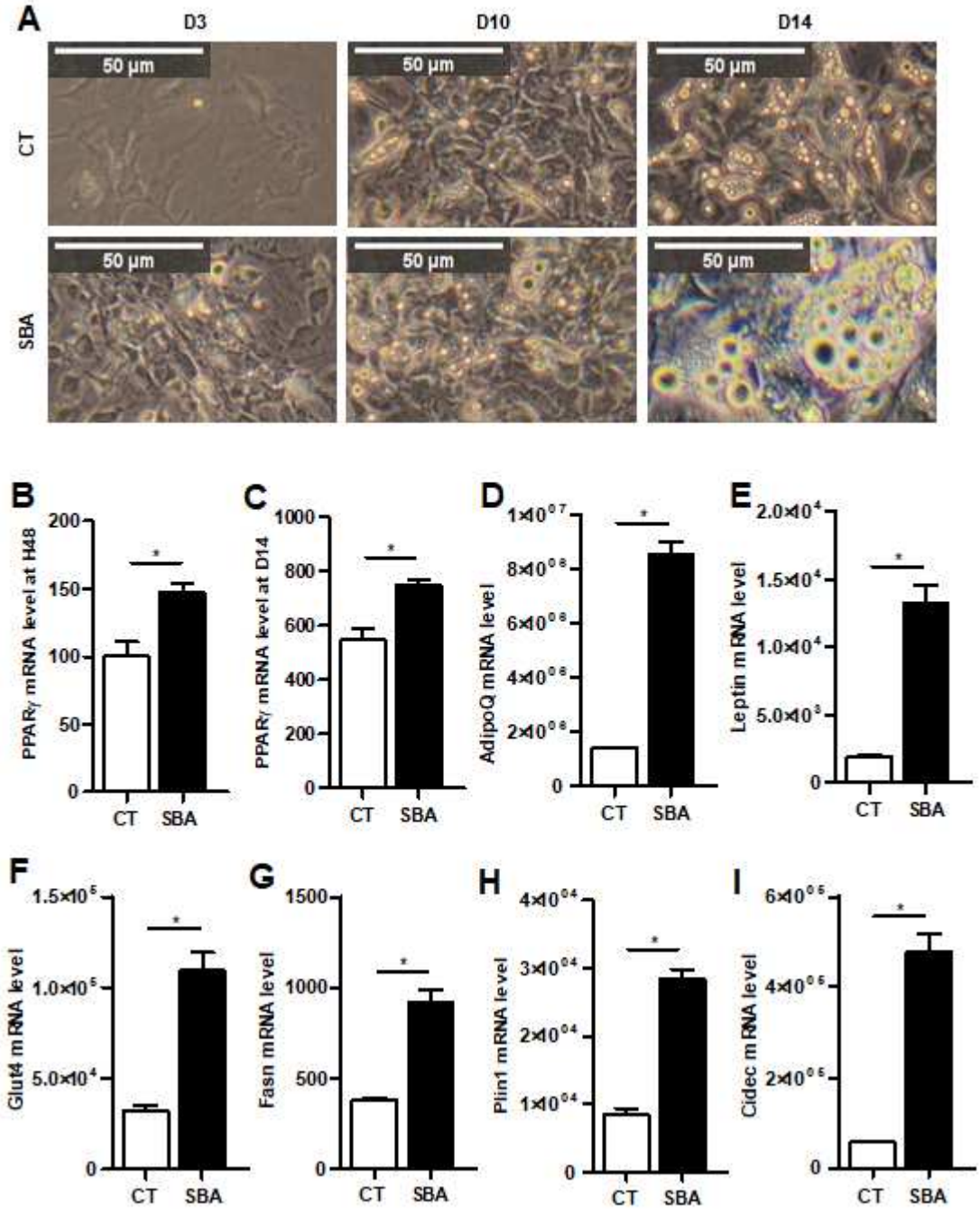

Fig. 3. Increase in adipogenesis induced by SBA protocol.

Microscopic observation of lipid droplets of bone marrow stromal cells (BMSCs) of CT and SBA mice after 3 days (D3), 10 days (D10) and 14 days (D14) of codifferentiation (A). Relative levels of mRNA adipocyte marker (*PPARγ2*) of BMSCs of SBA and CT mice cultured in a standard proliferative medium for 48 hours (B) or in the co-differentiation medium for 14 days (C). Relative mRNA levels of other adipocyte markers, adiponectin (*AdipoQ*) (D), *leptin* (E) and *glucose transporter type 4* (*Glut4*) (F) were determined on BMSCs of CT and SBA mice cultured for 14 days in the codifferentiation medium. Relative mRNA levels of genes related to lipid storage, fatty acid synthase (*Fasn*) (G), *perilipin of type*

1 (*Plin1*) (H) and *cell death inducing DFFA like effector C* (*Cidec*) (I) were measured after 14 days in the codifferentiation medium. Levels of adipocyte markers and genes related to lipid storage were reported to the mean of mRNA level of two housekeeping genes *Gapdh2*, and *18S* and expressed in percent of BMSCs of CT mice cultured in growth medium which refers to day 0 (70% of confluent cells). Representative data from four independent experiments depicted as means +/- S.E.M. are shown. $^{*}p<0.05$ vs. CT.

After 14 days of codifferentiation, functional tests of mineralization were performed by staining cells with alizarin red and quantifying the mineralized nodules by calculating a calcium to protein ratio (Fig. 4A). The results revealed that BMSCs from SBA mice displayed deeply altered osteoblastic functions, such as mineralization capabilities (-91%, $p<0.05$), compared to CT BMSCs. Interestingly, at this time point, BMSCs from SBA mice also displayed low mRNA levels of osteoblastic markers compared to what was observed in the BMSCs from CT mice: *Runx2* (-97%), *OSX* (-98%), *ALP* (-96%), and *OC* (-99%) (Fig. 4C-F). In addition, after just 48 hours of adhesion in a standard proliferative medium, the native unstimulated BMSCs from SBA mice already presented low levels of *Runx2* mRNA (-42%) than what was observed in BMSCs from CT mice (Fig. 4B).

Altogether, these results suggest an increase in adipogenesis at the expense of osteoblastogenesis in BMSCs from SBA mice and led us to suppose a preferential commitment of BMSCs from restricted mice to the adipogenic pathway.

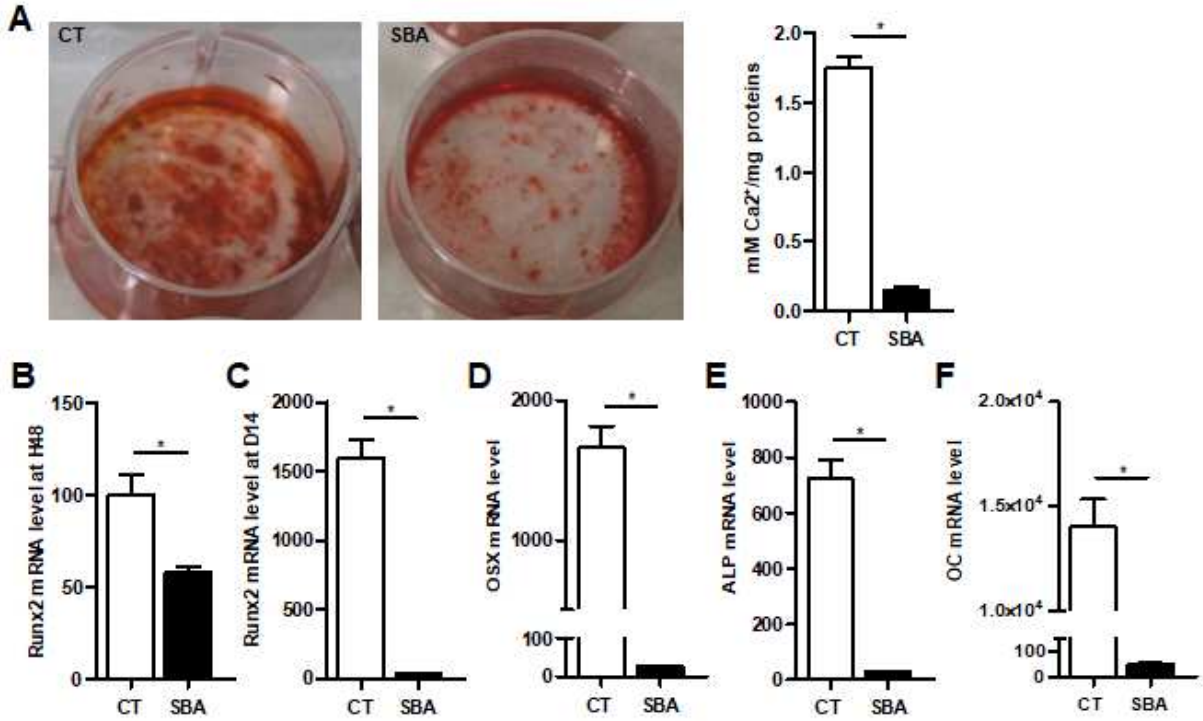

Fig. 4. Decrease of osteogenesis induced by SBA protocol.

Mineralization was highlighted by alizarin red staining and quantified by measuring the calcium to protein ratio (A). Relative mRNA levels of osteoblast marker (*Runx2*) of BMSCs of SBA and CT mice cultured in a standard proliferative medium for 48 hours (B) or in the codifferentiation medium for 14 days (C). Relative mRNA levels of osteoblast markers *osterix* (*OSX*) (D), *alkaline phosphatase* (*ALP*) (E) and *osteocalcin* (*OC*) (F) were determined on BMSCs of CT and SBA mice cultured for 14 days in the codifferentiation medium. Levels of these markers were reported as described previously in (Fig.3). Representative data from four independent experiments depicted as means +/- S.E.M. are shown. $^{*}p<0.05$ vs. CT.

3.3. Sirt1 is sustainably altered in BMSCs from SBA mice

It was recently demonstrated that adipogenic differentiation of SSCs requires substantial changes to chromatin organization [64]. In addition, given that HDAC proteins could be involved in chromatin compaction and genome stability [65,66], we hypothesized that these changes could occur in vivo in the BM of SBA mice. Thus, we measured the mRNA levels of HDACs known to be involved in the balance between adipocytic and osteoblastic differentiation. In BMSCs from SBA mice, neither the mRNA levels of *Sirt6* and *HDAC3*, which are known for their pro-osteoblastic effects [34,35,67], nor the mRNA levels of the pro-adipogenic factors *HDAC1* and *HDAC2* [36] were altered. This was observed in BMSCs from SBA mice after 48 hours of cell adhesion and 14 days of differentiation

(Supplemental Fig. S1A, B). Interestingly, the SBA protocol induced a substantial decrease in *Sirt1* mRNA levels in BMSCs (-75% vs CT BMSCs after 48 hours of culture; -96% vs CT BMSCs after 14 days of differentiation) (Fig. 5A, B), suggesting again that changes occurred *in vivo* and persisted *in vitro.*

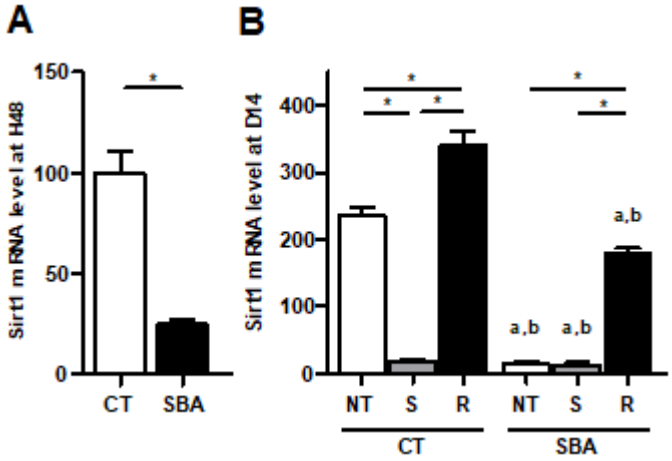

Fig. 5. SBA protocol induces a downregulation of *Sirt1* level which is normalized by resveratrol treatment

Relative levels of mRNA Sirt1 of BMSCs of SBA and CT mice cultured in a standard proliferative medium for 48 hours (A) or in the codifferentiation medium for 14 days (B). BMSCs of CT and SBA mice were treated for 14 days, in the codifferentiation medium, with 10µM of sirtinol (S) or 10µM of resveratrol (R) to study the effect of these treatments on Sirt1 expression. *Sirt1* levels were reported as previously described in (Fig.3). Representative data from four independent experiments depicted as means +/- S.E.M. are shown. $^{*}p<0.05$*;* a: $p<0.05$ vs CT not treated (NT); b: $p<0.05$ vs CT treated with sirtinol (s); c: $p<0.05$ vs CT treated with resveratrol (R).

Considering these results, the rest of the study was dedicated to studying the mechanisms by which Sirt1 could be involved in the regulation of BMSC differentiation in SBA mice. Other studies have shown that caloric restriction can stimulate the expression and activity of Sirt1 in various mammalian tissues, such as liver, white adipose tissue or calvaria [52,53]. Unfortunately, in the study on calvaria, neither BMA nor Sirt1 expression in long bones was assessed. Interestingly, it was also shown that caloric restriction decreases the mRNA level of *Sirt1* in the cerebellum and midbrain [54], suggesting a tissue-dependent regulation. Thus, to determine if there is a long bone-specific regulation of Sirt1 in SBA mice, the mRNA level of *Sirt1* was also assessed in subcutaneous adipose tissue and in liver. Significantly low levels of

Sirt1 mRNA were observed in subcutaneous adipose tissue from SBA mice (-86%), while there was no significant change in the liver (Supplemental Fig. S1C, D). These results demonstrated that the SBA protocol induced a decrease in the expression of Sirt1 in BMSCs and that there is a tissue-specific impact of energy deficit on this expression. This discrepancy between our results and others from Cohen et al [52] could be explained by changes in calorie or food restriction protocols, mice strain, their age and sex. Indeed, twelve-month-old male rats were used and calorie restriction means daily food allotment of 60% of that eaten by the ad-libitum animals immediately after weaning [52]. Whereas, in our study, seven-week-old female C57BL/6J were submitted to eight weeks of SBA protocol. Furthermore, the weight loss of mice in each protocol of calorie restriction could also explain this discrepancy. Indeed, contrary to our protocol which induces 18% of weight loss of mice, there is no information on weight loss in the study of Cohen et al [52].

Thus, one explanation for why there is a strong commitment of BMSCs towards the adipogenic pathway in SBA mice could be the loss of Sirt1 expression.

3.4. Sirt1 regulates BMA in the SBA model

To strengthen our results and to confirm the impact of Sirt1 on BMA in our model, we looked for mice expressing low levels of Sirt1 in BMSCs. Interestingly, our results demonstrated in BMSCs from mice floxed for *Sirt1*, a down regulation of 60% in mRNA level of *Sirt1* compared to their wild type. In addition, a decrease in Sirt1 protein expression was also found in these floxed mice (Fig. S2A-C). Thus, these mice displaying low levels of Sirt1 (LS) were further studied. This decreased Sirt1 expression was associated with an altered bone phenotype compared to the phenotype in WT mice (Supplemental Fig. S2D-H). Moreover, floxed mice displayed high BMA at the proximal tibia (+330% vs WT mice) (Fig. S2I). BMSCs from floxed mice displayed high mRNA levels of PPARγ at the expense of Runx2 after 48 hours of cell culture and after 14 days of codifferentiation (Fig. S2J-M). These results and those from other studies [42,53] confirmed the involvement of Sirt1 in regulating the osteoblast/adipocyte balance, and they confirmed that Sirt1 could be considered as an important regulator of bone mass.

To investigate the direct effect of Sirt1 on BMA in SBA mice, the expression and activity of Sirt1 were induced in 10-day organotypic cultures of tibias from CT and SBA mice. While tibias from SBA mice displayed low levels of *Sirt1* mRNA, resveratrol was used to increase *Sirt1* expression. Resveratrol at a 100 µM dose was selected as an efficient

concentration because it returned *Sirt1* mRNA levels in SBA tibias to CT levels (Supplemental Fig. S3A). Importantly, this recovery of Sirt1 levels also returned the BMA, BV/TV and Tb.Th in cultured tibias of SBA mice to normal levels, but it did not restore a normal cortical thickness (Supplemental Fig. S3B-H).

To test the direct effects of Sirt1 alterations on BMSCs from SBA mice, Sirt1 expression was induced by resveratrol treatment or repressed by sirtinol treatment of cultured BMSCs from CT and SBA mice. As shown in Fig. 5B, treatment with 10 μM sirtinol significantly decreased *Sirt1* mRNA levels in BMSCs from CT mice (-92%), while treatment with 10 μM resveratrol significantly increased *Sirt1* mRNA levels in BMSCs from SBA mice (+ 1164%). The decrease in *Sirt1* mRNA levels caused by sirtinol resulted in high mRNA levels for all adipocytic markers assessed in BMSCs from both CT and SBA mice. Indeed, in CT BMSCs *PPARγ* was 1.6-times higher after sirtinol treatment and in SBA BMSCs it was 1.5-times higher after this treatment. *Adiponectin* and *leptin* were 5-times higher in CT BMSCs and 1.4-times higher in SBA BMSCs than they were in untreated BMSCs from CT and SBA mice, respectively. *Glut4* was 3-times higher in CT BMSCs and 1.5-times higher in SBA BMSCs than it was in untreated BMSCs from CT and SBA mice, respectively (Fig. 6A-D).

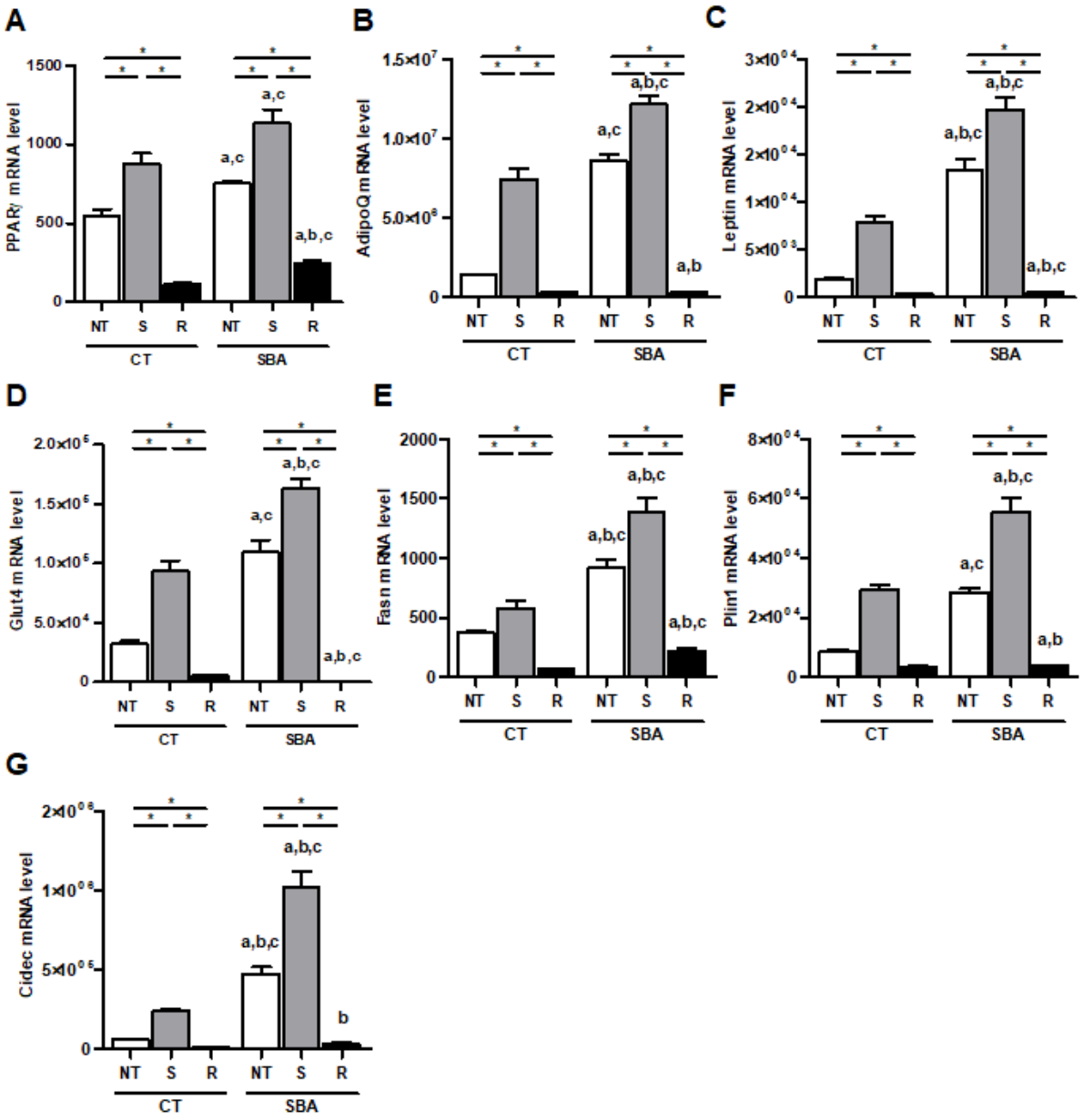

Fig. 6. Effects of sirtinol and resveratrol treatments on adipocytic markers and genes related to lipid storage

BMSCs of CT and SBA mice were treated with sirtinol (S) or resveratrol (R) in the same condition described in Fig.5 to study the effect of these treatments on adipocytic markers: *PPARγ2* (A), *AdipoQ* (B), *leptin* (C) and *Glut4* (D) and on genes related to lipid storage: *Fasn* (E) , *Plin1* (F) and *Cidec* (G). Levels of these markers were reported as described previously on Fig.3. Representative data from four independent experiments depicted as means +/- S.E.M. are shown. $^{*}p<0.05$ vs. CT. $^{*}p<0.05$; a: $p<0.05$ vs CT not treated (NT); b: $p<0.05$ vs CT treated with sirtinol (s); c: $p<0.05$ vs CT treated with resveratrol (R).

Following sirtinol treatment, an upregulation was also found for genes related to lipid storage: *Fasn* was 1.5-times higher in CT and SBA BMSCs than it was in untreated BMSCs from CT and SBA mice, respectively; *Plin1* was 3-times and 2-times higher in CT and SBA BMSCs than it was in untreated BMSCs of CT and SBA mice, respectively; and was *Cidec* 4-times and 2-times higher in CT and SBA BMSCs than it was in untreated BMSCs of CT and SBA mice, respectively. As expected, sirtinol treatment also induced low mineralization, as highlighted by red alizarin staining and the ratio of calcium to protein (3-times and 2-times lower in CT and SBA BMSCs than in untreated BMSCs from CT and SBA mice, respectively (Fig. 7A, B). This was associated with a low mRNA level of osteoblastic markers: *Runx2* level was 26-times lower only in CT BMSCs than it was in untreated BMSCs from CT mice; *OSX* level was 40-times and approximately 2-times lower in CT and SBA BMSCs than it was in untreated BMSCs of CT and SBA mice, respectively; *ALP* level was 11-times lower only in CT BMSCs than it was in untreated BMSCs from CT mice; and *OC* expression was 1.3-times and 2-times lower in CT and SBA BMSCs than it was in untreated BMSCs of CT and SBA mice, respectively (Fig. 7C-F). Unlike in BMSCs from CT mice, the mRNA levels of *Runx2* and *ALP* in BMSCs from SBA mice were not affected by sirtinol treatment, which is possibly because in these cells, the level of these genes was already extensively decreased by the energy deficit protocol (Fig. 7C and E). These findings are similar to those from many other studies. For example, it is demonstrated that sirtinol decreased the expression of osteoblast markers (*ALP*, *OSX*, and *Runx2*) in primary cells [68].

Interestingly, resveratrol treatment induced an increase in *Sirt1* mRNA to levels close to those of BMSCs from CT mice, although it was still significantly lower. Compared to untreated cells from the same mouse group, *Sirt1* mRNA levels were 1.4-times higher in CT BMSCs and 12.6-times higher in BMSCs from SBA mice after resveratrol exposure compared to levels without treatment (Fig. 5B). This stimulation of *Sirt1* expression by resveratrol led to a decrease in the mRNA levels of adipocytic markers. *PPARγ* was 4.7-times lower in CT BMSCs and 3.7-times lower in SBA BMSCs compared to untreated levels; *adiponectin* and *leptin* were approximately 5-times and 23-times lower in treated cells than in CT and SBA BMSCs, respectively; and *Glut 4* was 5-times and 127-times lower in CT and SBA BMSCs, respectively, when compared to the same cells without treatment (Fig. 6A-D). A downregulation was also induced by resveratrol for genes related to lipid storage: *Fasn* (approximately 5-times lower in CT and SBA BMSCs than in untreated BMSCs of CT and SBA mice, respectively), *Plin1* (approximately 2.5-times and 8-times lower in CT and SBA BMSCs than in untreated BMSCs from CT and SBA mice, respectively) and *Cidec* (6-times

and 16-times lower in CT and SBA BMSCs, respectively, than in BMSCs from CT and SBA mice, respectively) (Fig. 6E-G). In contrast, resveratrol treatment increased the level of osteoblastic markers *Runx2* (2-times and 11-times higher in CT and SBA BMSCs than in untreated BMSCs from CT and SBA mice, respectively), *OSX* (1.3-times and 8-times higher in CT and SBA BMSCs than in untreated BMSCs from CT and SBA mice, respectively), *ALP* (1.3-times and 15-times higher in CT and SBA BMSCs than in untreated BMSCs from CT and SBA mice, respectively) and *OC* (1.6-times and 2.6-times higher in CT and SBA BMSCs than in untreated BMSCs from CT and SBA mice, respectively) (Fig. 7C-F). Resveratrol induced an increase in mineralization in both CT and SBA BMSCs, as shown by high levels of red alizarin staining and a high calcium to protein ratio compared to untreated BMSCs (1.3-times and 11-times higher in CT and SBA BMSCs than in untreated BMSCs from CT and SBA mice, respectively) (Fig. 7A-B). Altogether, these results show that in BMSCs, downregulation of Sirt1 recapitulated most of the changes induced by the SBA protocol, and the Sirt1 downregulation induced by sirtinol made the SBA protocol-induced alterations in BMSCs even worse. Moreover, resveratrol enhanced Sirt1 expression and reversed the strong adipogenic commitment of BMSCs from SBA mice.

It is also reported that Sirt1 activators improve whole-body glucose homeostasis and insulin sensitivity in adipose tissue, skeletal muscle and liver [69]. Conversely, *Sirt1*-/- mice or their isolated islets show blunted insulin secretion [70]. In addition, transgenic mice generated by knocking in Sirt1 cDNA into the β-actin locus displayed increased Sirt1 expression and a decrease in blood adipokines, cholesterol, insulin and fasted glucose [37]. Sirt1 was also involved in fat metabolism regulation. Indeed, in white adipose tissue (WAT), Sirt1 could act as a PPARγ repressor leading to fat mobilization instead of storage [71]. Sirt1 could repress PPARγ transcriptional activity on target lipogenic genes directly through deacetylation [72]. Overexpression of human Sirt1 protects mice again stage-related glucose intolerance [73]. This effect was concomitant with a prevention of fat accumulation in peripheral tissues and a higher ability of WAT to trigger lipolysis and fat oxidation [73]. All these data demonstrate that Sirt1 have beneficial effects on glucose homeostasis and insulin sensitivity and Sirt1 has a major role in preventing excessive fat accumulation and enhancing the ability of the tissue to respond to lipolytic stimuli.

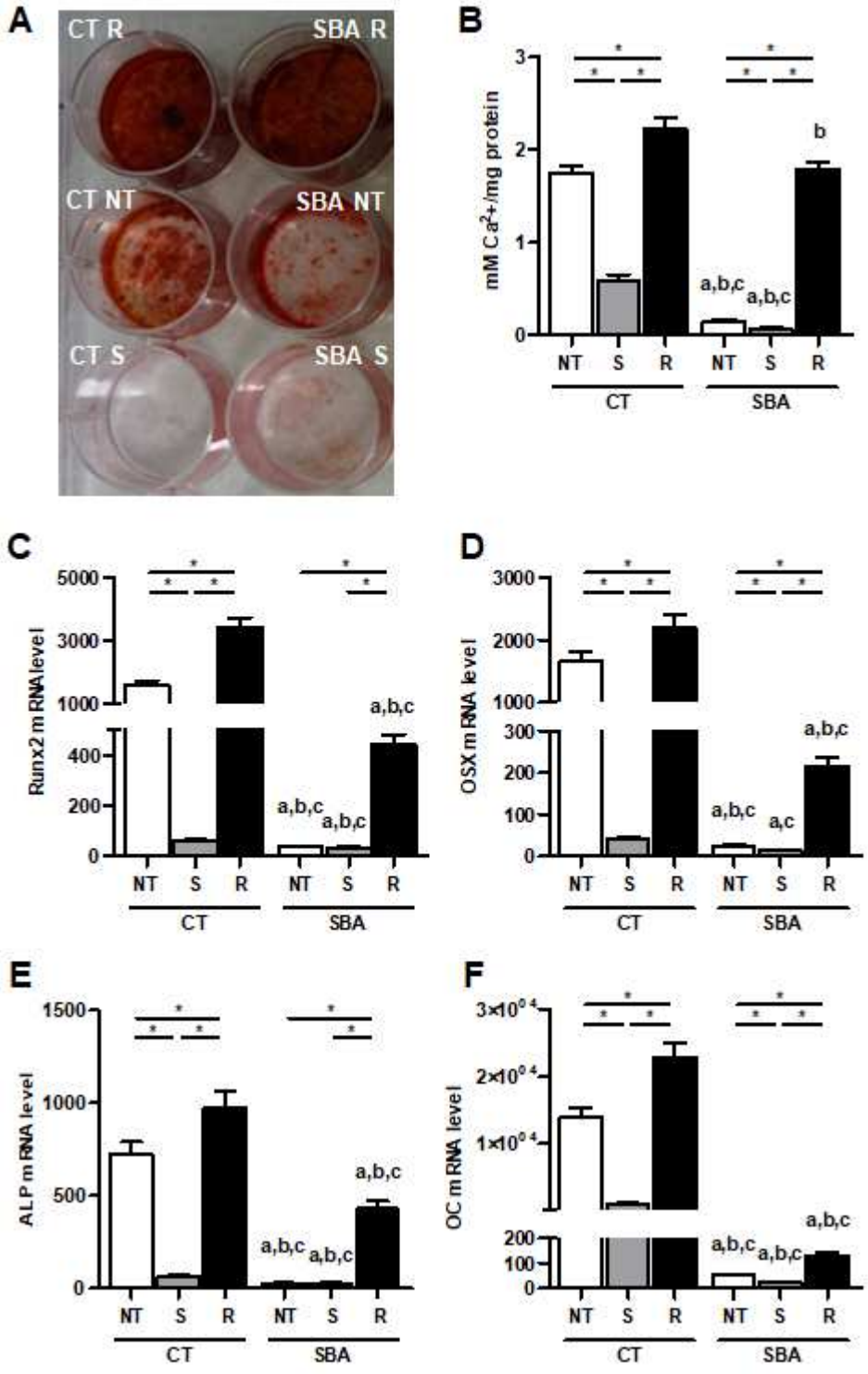

Fig. 7. Effects of sirtinol and resveratrol treatments on osteoblastic markers

Mineralization was highlighted by alizarin red staining (A) and quantified by measuring the calcium to protein ratio (B) after treatment of BMSCs from CT and SBA mice with 10µM of sirtinol (S) or resveratrol (R). BMSCs from CT and SBA mice were treated with sirtinol (S) or resveratrol (R) in the same condition described in Fig.5 to study the effect of these treatments on osteoblastic markers: *Runx2* (C), *OSX* (D), *ALP* (E) and *OC* (F). Levels of these markers

were reported as described previously in Fig.3. Representative data from four independent experiments depicted as means +/- S.E.M. are shown. $^{*}p<0.05$ vs. CT. $^{*}p<0.05$; a: $p<0.05$ vs CT not treated (NT); b: $p<0.05$ vs CT treated with sirtinol (s); c: $p<0.05$ vs CT treated with resveratrol (R).

3.5. Low levels of Sirt1 in BMSCs from SBA mice are associated with high levels of Runx2 and Foxo1 acetylation

Among the Foxo family, it was reported that Foxo1 could play an important role in bone formation *in vivo* by modulating the proliferation of osteoblastic precursors [74]. Foxo1 has been shown to affect the differentiation of adipocytes [75,76]. Constitutively active Foxo1 inhibits the differentiation of pre-adipocytes into mature adipocytes, while a dominant-negative Foxo1 enhances adipocyte differentiation [75]. Moreover, chromatin immunoprecipitation assays revealed a direct interaction between Foxo1 and the Runx2 promoter [77], providing a mechanism by which Foxo1 may modulate osteoblast differentiation. It was also shown that deacetylation of Foxo1 by Sirt1 suppresses osteoclastogenesis [78]. Runx2 was also shown to be activated by Sirt1-induced deacetylation [45].

Therefore, to investigate the molecular mechanisms by which Sirt1 could regulate osteogenesis in the SBA model, the acetylation levels of Runx2 and Foxo1 transcription factors were determined. The SBA protocol induced a decrease in the Sirt1 protein level in BMSCs (Fig. 8A, B). This decrease was accompanied by a high level of acetylation of both Runx2 and Foxo1 transcription factors (Fig. 8C, D).

Furthermore, sirtinol-induced Sirt1 protein decrease in both BMSCs from experimental and CT mice (Fig. 8A, B) was accompanied by high acetylation levels of Runx2 and Foxo1 transcription factors (Fig. 8C, D). Interestingly, Runx2 and Foxo1 acetylation was strongly decreased by resveratrol induced Sirt1 protein activation in BMSCs from SBA and CT mice. (Fig. 8A-D). These findings confirmed data from Shakibaei et al [45], which showed that resveratrol-mediated modulation of Sirt1/Runx2 promotes osteogenic differentiation of mesenchymal stem cells [45]. Furthermore, immunoprecipitation and western blotting demonstrated functional and physical interactions between Runx2 and Sirt1, suggesting that Sirt1 directly deacetylates Runx2 [45]. Concerning the appearance of the double band in the western blot of Sirt1 in our model, it is described that Sirt1 can have two isoforms: isoform 1 and isoform 2 [79]. Thus this double band could be due to the two isoforms of Sirt1 protein.

Our data show that a chronic energy deficiency in female mice causes a decrease in Sirt1 levels and a decrease in BMSC activity, resulting in critical changes to Runx2 and Foxo1 acetylation levels and thus to their activity.

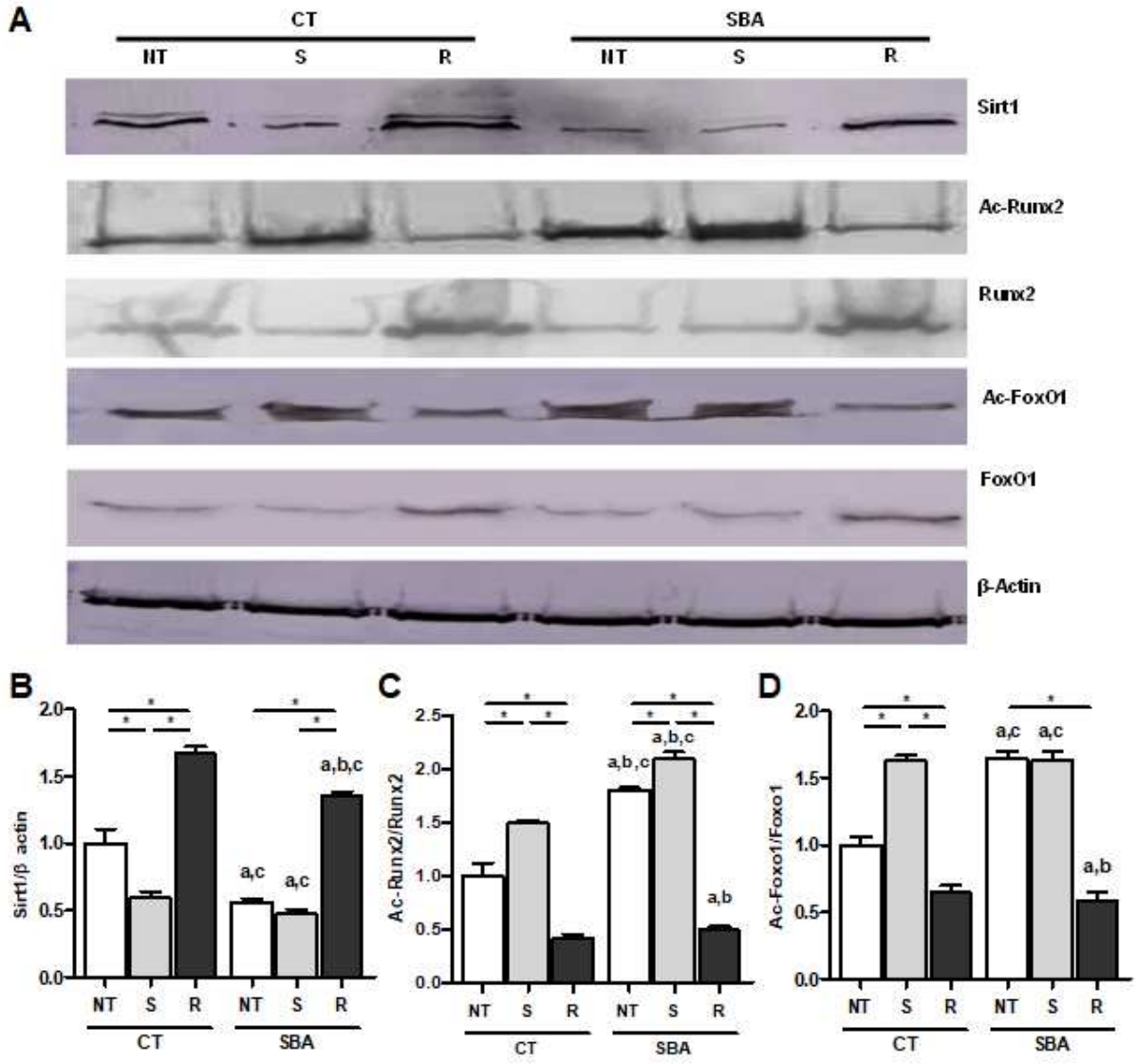

Fig. 8. Effects of sirtinol and resveratrol on Sirt1, Foxo1 and Runx2 acetylation

Proteins are extracted from BMSCs of CT and SBA mice cultured in the same conditions as mentioned in Fig.7. A: Western blot analysis of Sirt1, acetylated Runx2 (Ac-Runx2), total Runx2, acetylated Foxo1 (Ac-Foxo1), total Foxo1 and β-actin. B-D: qualitative measure of immunoblots of Sirt1 to β-actin ratio, Ac-Foxo1 to Foxo1 ratio and Ac-Runx2 to Runx2 ratio by densitometry (Bio Rad, GS-800 calibrated densitometer). Representative data from four independent experiments depicted as means +/- S.E.M. are shown. $^{*}p<0.05$ vs. CT. $^{*}p<0.05$;

a: $p<0.05$ vs CT not treated (NT); b: $p<0.05$ vs CT treated with sirtinol (s); c: $p<0.05$ vs CT treated with resveratrol (R).

4. Conclusion

In summary, this study demonstrates that a chronic energy deficiency in female mice induces a low bone mass and a high BMA. BMSCs isolated from SBA mice are characterized by high expression of markers from the adipocytic lineage at the expense of those from the osteoblastic lineage. This imbalance is also found when testing the differentiation capacities of these cells, and it is associated with a decrease in the expression and activity of Sirt1. It has also been demonstrated that (i) Sirt1 regulates BMA in SBA mice, which we showed by investigating the consequences of implementing the SBA protocol on Sirt1-deficient mice, and (ii) in vitro, a low level of Sirt1 is responsible for alterations in the differentiation capacities of BMSCs. Finally, the study shows that Sirt1 acts on BMSC differentiation in SBA mice through the regulation of Runx2 and Foxo1 acetylation. Furthermore, given the beneficial effects of resveratrol on bone microarchitecture and BMA in organotypic culture of tibias from CT and SBA mice after only 10 days, these data may present a new therapeutic strategy for preventing or treating osteoporosis related to AN by acting on the expression and activity of Sirt1. All these data suggest that Sirt1 could be considered a potential therapeutic target in osteoporosis related to AN. Thus using Sirt1 as a therapeutic tool probably means to check for several kinds of side effects. However, resveratrol was already used to treat patients for neurologic or metabolic alterations [80-82].

The perspective of this study is to assess epigenetic alterations of chromatin in BMSCs from SBA mice. The results would elucidate the involvement of this additional Sirt1 mechanism of action in this model, and as a result, it would determine if the direct action of Sirt1 on transcriptional regulators shown here is associated with a broader action at the chromatin level.

Funding

This work is supported by grants from Société Française de Rhumatologie (SFR), Région Hauts-de-France (France) and Université du Littoral Côte d'Opale, Dunkerque, France.

Declaration of Competing Interest

The authors stated that they have no conflicts of interest.

Author contributions:

Loïc Louvet: participated in the conception and design of the study, performed data interpretation and analysis, maintained the cell cultures, performed biochemical characterizations and real-time PCR experiments and drafted the manuscript. Damien Leterme: participated in the writing of the protocol to obtain a permit number from the Committee on the Ethics of Animal Experiments and obtain all samples taken during mouse sacrifices. Séverine Delplace: participated in histological analysis to determine the density of bone marrow adipocytes. Flore Miellot: participated in the µ-CT analysis. Pierre Marchandise: performed all µ-CT scans. Véronique Gauthier: participated in animal housing and care and histological analysis. Pierre Hardouin: participated in the design of the project. Olfa Ghali Mhenni and Christophe Chauveau: principal investigators, conceived and designed the study, participated in data analysis and interpretation and in drafting of the manuscript. All authors read and approved the final manuscript.

References

[1] S. Ahdjoudj, F. Lasmoles, X. Holy, E. Zerath, P.J. Marie, Transforming growth factor beta2 inhibits adipocyte differentiation induced by skeletal unloading in rat bone marrow stroma, J Bone Miner Res. 17 (4) (2002) 668–677.

[2] J. Justesen, K. Stenderup, E.N. Ebbesen, L. Mosekilde, T. Steiniche, M. Kassem , Adipocyte tissue volume in bone marrow is increased with aging and in patients with osteoporosis, Biogerontology, 2 (3) (2001) 165–171.

[3] S. Verma, J.H. Rajaratnam, J. Denton, J.A. Hoyland, R.J. Byers, Adipocytic proportion of bone marrow is inversely related to bone formation in osteoporosis, J Clin Pathol. 55 (9) (2002) 693–698.

[4] S. Botolin, L.R. McCabe, Bone loss and increased bone adiposity in sponta-neous and pharmacologically induced diabetic mice, Endocrinology 148 (1) (2007) 198–205.

[5] M.A. Piccinin, Z.A. Khan, Pathophysiological role of enhanced bone marrow adipogenesis in diabetic complications, Adipocyte 3 (4) (2014) 263–272.

[6] A.L. Schafer, X. Li, A.V. Schwartz, L.S. Tufts, A.L. Wheeler, C. Grunfeld C, L. Stewart, S.J. Rogers, J.T. Carter, A.M. Posselt, D.M. Black, D.M. Shoback, Changes in vertebral bone marrow fat and bone mass after gastric bypass surgery: a pilot study, Bone 74 (2015) 140–145.

[7] M.A. Bredella, M. Torriani,R.H. Ghomi, B.J. Thomas, D.J. Brick, A.V. Gerweck, C.J. Rosen, A. Klibanski, K.K. Miller, Vertebral bone marrow fat is positively associated with visceral fat and inversely associated with IGF-1 in obese women, Obesity (Silver Spring) 19 (1) (2011) 49–53.

[8] M.A. Bredella, P.K. Fazeli, K.K. Miller, M. Misra, M. Torriani, B.J. Thomas R.H. Ghomi, C.J. Rosen, A. Klibanski, Increased bone marrow fat in anorexia nervosa, J Clin Endocrinol Metab 94 (6) (2009) 2129–2136.

[9] E. Abella, E. Feliu, I. Granada, F. Millá, A. Oriol, J.M. Ribera, L. Sánchez-Planell, L.I. Berga, J.C. Reverter, C. Rozman, Bone marrow changes in anorexia nervosa are correlated with the amount of weight loss and not with other clinical findings, Am J Clin Pathol 118 (2002) 582–588.

[10] K. Ecklund, S. Vajapeyam, H.A. Feldman, C.D. Buzney, R.V. Mulkern, P.K. Kleinman, C.J. Rosen, C.M. Gordon, Bone marrow changes in adolescent girls with anorexia nervosa, J Bone Miner Res 25 (2010) 298–304.

[11] M.A. Bredella, P.K. Fazeli, S.M. Daley, K.K. Miller, C.J. Rosen, A. Klibanski, M. Torriani, Marrow fat composition in anorexia nervosa, Bone 66 (2014) 199–204.

[12] P.K. Fazeli, M.A. Bredella, L. Freedman, B.J. Thomas, A. Breggia, E. Meenaghan, C.J. Rosen, A. Klibanski, Marrow fat and preadipocyte factor-1 levels decrease with recovery in women with anorexia nervosa, J Bone Miner Res 27 (9) (2012) 1864–1871.

[13] S. Badr, I. Legroux-Gérot, J. Vignau, C. Chauveau, S. Ruschke, D.C. Karampinos, J.F Budzik, B. Cortet, A. Cotten, Comparison of regional bone marrow adiposity characteristics at the hip of underweight and weight-recovered women with anorexia nervosa using magnetic resonance spectroscopy, Bone 127 (2019) 135-145.

[14] S.G. Moore, K.L. Dawson, Red and yellow marrow in the femur: age-related changes in appearance at MR imaging, Radiology 175 (1) (1990) 219–223.

[15] J.F. Griffith, D.K.W. Yeung, H.T. Ma, J.C.S. Leung, T.C.Y. Kwok, P.C. Leung, Bone marrow fat content in the elderly: a reversal of sex difference seen in younger subjects, J Magn Reson Imaging 36 (1) (2012) 225–230.

[16] W. Shen, J. Chen, M. Gantz, M. Punyanitya, S.B. Heymsfield, D. Gallagher, J. Albu, E. Engelson, D. Kotler, X. Pi-Sunyer, V. Gilsanz, MRI-measured pelvic bone marrow adipose tissue is inversely related to DXA- measured bone mineral in younger and older adults, Eur J Clin Nutr 66 (9) (2012) 983–938.

[17] T.A.L. Wren, S.A. Chung, F.J. Dorey, S. Bluml, G.B. Adams, V. Gilsanz., Bone marrow fat is inversely related to cortical bone in young and old subjects, J Clin Endocrinol Metab 96 (3) (2011) 782–786.

[18] C.J. Rosen, M.L.Bouxsein, Mechanisms of disease: is osteoporosis the obesity of bone? Nat Clin Pract Rheumatol. 2 (1) (2006) 35-43.

[19] P.K. Fazeli, M.C. Horowitz, O.A. MacDougald, E.L. Scheller, M.S. Rodeheffer, C.J. Rosen, A. Klibanski, Marrow fat and bone--new perspectives, J Clin Endocrinol Metab 98 (3) (2013) 935-945.

[20] M.E. Nuttall, F. Shah, V. Singh, C. Thomas-Porch, T. Frazier, J.M. Gimble, Adipocytes and the regulation of bone remodeling: a balancing act, Calcif Tissue Int. 94 (1) (2014) 78-87.

[21] J.A. Fretz, T. Nelson, Y. Xi, D. J. Adams, C.J. Rosen, M.C. Horowitz, Altered metabolism and lipodystrophy in the early B-cell factor 1-deficient mouse, Endocrinology. 151 (4) (2010) 1611-1621.

[22] A. Elbaz, X. Wu, D. Rivas, J.M. Gimble, G. Duque. Inhibition of fatty acid biosynthesis prevents adipocyte lipotoxicity on human osteoblasts in vitro, J Cell Mol Med 14 (4) (2010) 982–991.

[23] R. Nishimura, K. Hata, F. Ikeda, F. Ichida, A. Shimoyama, T. Matsubara, M. Wada, K. Amano, T. Yoneda, Signal transduction and transcriptional regulation during mesenchymal cell differentiation, J Bone Miner Metab. 26 (3) (2008) 203–212.

[24] M. Owen, Marrow stromal stem cells, J Cell Sci (Supplement) (10) (1988) 63–76.

[25] M.F. Pittenger, A.M. Mackay, S.C. Beck, R.K. Jaiswal, R. Douglas, J.D. Mosca, M.A. Moorman, D.W. Simonetti, S. Craig, D.R. Marshak, Multilineage potential of adult human mesenchymal stem cells, Science 284 (5411) (1999)143–147.

[26] J.N. Beresford, J.H. Bennett, C. Devlin, P.S. Leboy, M.E. Owen, Evidence for an inverse relationship between the differentiation of adipocytic and osteogenic cells in rat marrow stromal cell cultures, J Cell Sci.102 (Part 2) (1992) 341–351.

[27] E.J. Moerman, K. Teng, D.A. Lipschitz, B. Lecka-Czernik, Aging activates adipogenic and suppresses osteogenic programs in mesenchymal marrow stroma/stem cells: the role of PPAR-gamma2 transcription factor and TGF-beta/BMP signaling pathways, Aging Cell. 3 (6) (2004) 379-389.

[28] L. Song, M. Liu, N. Ono, F.R. Bringhurst, H.M. Kronenberg, J. Guo, Loss of wnt/β-catenin signaling causes cell fate shift of preosteoblasts from osteoblasts to adipocytes, J Bone Miner Res. 27 (11) (2012) 2344-2358.

[29] J. Skillington, L. Choy, R. Derynck, Bone morphogenetic protein and retinoic acid signaling cooperate to induce osteoblast differentiation of preadipocytes, J Cell Biol 159 (1) (2002) 135-146.

[30] J. Li, N. Zhang, X. Huang, J. Xu, J.C. Fernandes, K. Dai, X. Zhang, Dexamethasone shifts bone marrow stromal cells from osteoblasts to adipocytes by C/EBPalpha promoter methylation, Cell Death Dis 4(:e832) (2013).

[31] O. Ghali, O. Broux, G. Falgayrac, N. Haren, J. PTM van Leeuwen, G. Penel, P. Hardouin, C. Chauveau, Dexamethasone in osteogenic medium strongly induces adipocyte differentiation of mouse bone marrow stromal cells and increases osteoblast differentiation, BMC Cell Biology (2015) 16-19.

[32] E.W. Bradley, M.E. McGee-Lawrence, J.J. Westendorf, Hdac-mediated control of endochondral and intramembranous ossification, Crit Rev Eukaryot Gene Expr. 21 (2) (2011) 101–113.

[33] M.E. McGee-Lawrence, L. R. Carpio, R.J. Schulze, J. L. Pierce, M. A. McNiven, J. N. Farr, S. Khosla, M. Jo Oursler, J. J. Westendorf , Hdac3 Deficiency Increases Marrow Adiposity and Induces Lipid Storage and Glucocorticoid Metabolism in Osteochondroprogenitor Cells, J Bone Miner Res 31 (1) (2016) 116–128.

[34] D.F. Razidlo, T.J. Whitney, M.E. Casper, M.E. McGee-Lawrence, B.A. Stensgard, X. Li, F.J. Secreto, S.K. Knutson, S.W. Hiebert, J.J. Westendorf, Histone deacetylase 3 depletion in osteo/chondroprogenitor cells decreases bone density and increases marrow fat, PLoS One 5 (7) (2010) e11492.

[35] M.E. McGee-Lawrence, E.W. Bradley, A. Dudakovic, S.W. Carlson, Z.C. Ryan, R. Kumar, M. Dadsetan, M.J. Yaszemski, Q. Chen, A. KN, J.J. Westendorf, Histone deacetylase 3 is required for maintenance of bone mass during aging, Bone 52 (1) (2013) 296–307.

[36] M. Haberland, M. Carrer, M.H. Mokalled, R.L. Montgomery, E.N. Olson, Redundant control of adipogenesis by histone deacetylases 1 and 2, J Biol Chem 285 (19) (2010) 14663–14670.

[37] L. Bordone, D. Cohen, A. Robinson, M.C. Motta, E. van Veen, A. Czopik , A.D. Steele, H. Crowe, S. Marmor, J. Luo, W. Gu, L. Guarente, SIRT1 transgenic mice show phenotypes resembling calorie restriction, Aging Cell 6 (2007) 759–767.

[38] G. Donmez, D. Wang, D.E. Cohen, L. Guarente, SIRT1 suppresses_-amyloid production by activating the _-secretase gene ADAM10, Cell 142 (2010) 320–332.

[39] H. Artsi, E. Cohen-Kfir, I. Gurt, R. Shahar, A. Bajayo, N. Kalish, T. M. Bellido, Y. Gabet, R. Dresner-Pollak, The sirtuin 1 activator SRT3025 Down-Regulates Sclerostin and Rescues Ovarectomy-Induced Bone Loss and Biomechanical Deterioration in Female Mice, Endocrinology 155 (9) (2014) 3508-3515.

[40] D. Herranz, M. Cañamero, F. Mulero, B. Martinez-Pastor, O. Fernandez-Capetillo, M. Serrano, Sirt1 improves healthy ageing and protects from metabolic syndrome-associated cancer syndrome, Nat Commun (2010) 1: 3

[41] S. Iyer, L. Han, S. M. Bartell, H. N. Kim, I. Gubrij, R. de Cabo, C. A. O'Brien, S. C. Manolagas, M. Almeida, Sirtuin1 (Sirt1) Promotes Cortical Bone Formation by Preventing β-Catenin Sequestration by FoxO Transcription Factors in Osteoblast Progenitors, J Biol Chem 289 (35) (2014) 24069–24078.

[42] E. Cohen-Kfir, H. Artsi, A. Levin, E. Abramowitz, A. Bajayo, I. Gurt, L. Zhong, A. D'Urso, D. Toiber, R. Mostoslavsky, R. Dresner-Pollak**.** Sirt1 is a regulator of bone mass and a repressor of Sost encoding for sclerostin, a bone formation inhibitor, Endocrinology 152 (12) (2011) 4514-4524.

[43] C.M. Backesjo, Y. Li, U. Lindgren, L.A. Haldosen, Activation of Sirt1 decreases adipocyte formation during osteoblast differentiation of mesenchymal stem cells, Cells Tissues Organs 189(1–4) (2009) 93–97.

[44] P. Simic, K. Zainabadi, E. Bell, D.B. Sykes, B. Saez, S. Lotinun, R. Baron, D. Scadden, E. Schipani, L. Guarente, SIRT1 regulates differentiation of mesenchymal stem cells by deacetylating β-catenin, EMBO Mol Med 5 (3) (2013) 430-440.

[45] M. Shakibaei, P. Shayan, F. Busch, C. Aldinger, C. Buhrmann, C. Lueders, A. Mobasheri, Resveratrol Mediated Modulation of Sirt-1/Runx2 Promotes Osteogenic Differentiation of Mesenchymal Stem Cells: Potential Role of Runx2 Deacetylation, PLoS One 7 (4) (2012).

[46] P.C. Tseng, S.M. Hou, R.J. Chen, H.W. Peng, C.F. Hsieh, M.L. Kuo, M.L.Yen, Resveratrol promotes osteogenesis of human mesenchymal stem cells by upregulating RUNX2 gene expression via the SIRT1/FOXO3A axis, J Bone Miner Res 26 (2011) 2552–2563.

[47] T. Finkel, C.X. Deng, R. Mostoslavsky**,** Recent progress in the biology and physiology of sirtuins, Nature 460 (2009) 587–591.

[48] K. Mizutani, K. Ikeda, Y. Kawai, Y. Yamori, Resveratrol stimulates the proliferation and differentiation of osteoblastic MC3T3-E1 cells, Biochem Biophys Res Commun 253 (3) (1998) 859-863.

[49] L.H. Song, W. Pan, Y.H. Yu, L.D. Quarles, H.H. Zhou, Z.S. Xiao, Resveratrol prevents CsA inhibition of proliferation and osteoblastic differentiation of mouse bone marrow-derived mesenchymal stem cells through an ER/NO/cGMP pathway, Toxicol In Vitro 20 (6) (2006) 915-22.

[50] C. Botti, I. Caiafa, A. Coppola, F. Cuomo, M. Miceli, L. Altucci, G. Cobellis, SIRT1 inhibition affects angiogenic properties of human MSCs, Biomed Res Int (2014).

[51] A. Orecchia, C. Scarponi, F. Di Felice, E. Cesarini, S. Avitabile, A. Mai, M.L. Mauro, V. Sirri, G. Zambruno, C. Albanesi, G. Camilloni, C.M. Failla. Sirtinol treatment reduces inflammation in human dermal microvascular endothelial cells, PLoS One 6 (9): e24307 (2011).

[52] H.Y. Cohen, C. Miller, K.J. Bitterman, N.R. Wall, B. Hekking, B. Kessler, K.T. Howitz, M. Gorospe, R. de Cabo, D.A. Sinclair, Calorie restriction promotes mammalian cell survival by inducing the SIRT1 deacetylase, Science. 305 (5682) (2004) 390-392.

[53] K. Zainabadi, C.J. Liu, A.L.M. Caldwell, L. Guarente, SIRT1 is a positive regulator of in vivo bone mass and a therapeutic target for osteoporosis, PLoS One 12 (9) :e0185236 (2017).

[54] D. Chen, A.D. Steele, G. Hutter, J. Bruno, A. Govindarajan, E. Easlon, S.J. Lin, A. Aguzzi, S. Lindquist, L. Guarente, The role of calorie restriction and SIRT1 in prion-mediated neurodegeneration, Exp Gerontol. 43 (12) (2008) 1086-1093.

[55] S. Zgheib, M. Méquinion, S. Lucas, D. Leterme, O. Ghali,V. Tolle, P. Zizzari, N. Bellefontaine, I. Legroux-Gérot, P. Hardouin, O. Broux, O. Viltart, C. Chauveau, Long-Term Physiological Alterations and Recovery in a Mouse Model of Separation Associated with Time- Restricted Feeding: A Tool to Study Anorexia Nervosa Related Consequences, PLoS One 9 (8):e103775 (2014).

[56] O. Ghali, C. Chauveau, P. Hardouin, O. Broux, J.C. Devedjian, TNF-alpha's effects on proliferation and apoptosis in human mesenchymal stem cells depend on RUNX2 expression, J Bone Miner Res 25 (7) (2010)1616–1626.

[57] X. Coutel, C. Olejnik, P. Marchandise, J. Delattre, H. Béhal, G. Kerckhofs, G. Penel, A Novel microCT Method for Bone and Marrow Adipose Tissue Alignment Identifies Key Differences Between Mandible and Tibia in Rats, Calcif Tissue Int 103 (2) (2018) 189-197.

[58] M.J. Devlin, A.M. Cloutier, N.A. Thomas, D.A. Panus, S. Lotinun, I. Pinz, R. Baron, C.J. Rosen , M.L. Bouxsein, Caloric restriction leads to high marrow adiposity and low bone mass in growing mice, J Bone Miner Res 25 (9) (2010)2078–2088.

[59] W.P. Cawthorn, E.L. Scheller, S.D. Parlee, H.A. Pham, B.S. Learman, C.M. Redshaw, R.J. Sulston, A.A. Burr, A.K. Das, B.R. Simon, H. Mori, A.J. Bree, B. Schell, V. Krishnan, O.A. MacDougald, Expansion of bone marrow adipose tissue during caloric restriction is associated with increased circulating glucocorticoids and not with hypolep- tinemia, Endocrinology 157 (2) (2016) 508–521.

[60] K. Baek, S.A. Bloomfield, Blocking β-adrenergic signaling attenuates reductions in circulating leptin, cancellous bone mass, and marrow adiposity seen with dietary energy restriction, J Appl Physiol 113 (11) (1985) 1792–801.

[61] M.W. Hamrick, K.H. Ding, S. Ponnala, S.L. Ferrari, C.M. Isales, Caloric restriction decreases cortical bone mass but spares trabecular bone in the mouse skeleton: implications for the regulation of bone mass by body weight, J Bone Miner Res 23 (6) (2008) 870–878.

[62] P. Bianco, P.G. Robey, I. Saggio, M. Riminucci, "Mesenchymal" stem cells in human bone marrow (skeletal stem cells): a critical discussion of their nature, identity, and significance in incurable skeletal disease, Hum Gene Ther 21 (2010) 1057–1066.

[63] S. Muruganandan, A.A. Roman, C.J. Sinal, Adipocyte differentiation of bone marrow-derived mesenchymal stem cells: cross talk with the osteoblastogenic program, Cell Mol Life Sci 66 (2009) 236–253.

[64] A. Rauch, A.K. Haakonsson, J.G.S. Madsen, M. Larsen, I. Forss, M.R. Madsen, E.L. Van Hauwaert, C. Wiwie, N.Z. Jespersen, M. Tencerova, R. Nielsen, B.D. Larsen, R. Röttger, J. Baumbach, C. Scheele, M. Kassem, S. Mandrup, Osteogenesis depends on commissioning of a network of stem cell transcription factors that act as repressors of adipogenesis, Nat Genet 51 (4) (2019) 716-727.

[65] X. Wu, N. Cao, M. Fenech, X. Wang, Role of Sirtuins in Maintenance of Genomic Stability: Relevance to Cancer and Healthy Aging, DNA Cell Biol. 35(10) (2016) 542-575.

[66] S.Y. Kim, C.K. Sim, H. Tang, W Han, K. Zhang, F. Xu, Acetylome study in mouse adipocytes identifies targets of SIRT1 deacetylation in chromatin organization and RNA processing, Arch Biochem Biophys 598 (15) (2016) 1-10.

[67] T. Sugatani, O. Agapova, H.H. Malluche, K.A. Hruska, SIRT6 deficiency culminates in low-turnover osteopenia, Bone 81 (2015)168-177.

[68] Y.M. Lee, S.I. Shin, K.S. Shin, Y.R. Lee, B.H. Park, E.C. Kim, The role of sirtuin 1 in osteoblastic differentiation in human periodontal ligament cells, J Periodontal Res 46 (6) (2011) 712-721.

[69] J.C. Milne, P.D. Lambert, S. Schenk, D.P. Carney, J.J. Smith, D.J. Gagne, L. Jin, O. Boss, R.B. Perni, C.B. Vu, J.E. Bemis, R. Xie, J.S. Disch, P.Y. Ng, J.J. Nunes, A.V. Lynch, H. Yang, H. Galonek, K. Israelian, W. Choy, A. Iffland, S. Lavu, O. Medvedik, D.A. Sinclair, J.M. Olefsky, M.R. Jirousek, P.J. Elliott, C.H. Westphal, Small molecule activators of SIRT1 as therapeutics for the treatment of type 2 diabetes, Nature 29;450(7170) (2007) 712-716.

[70] L. Bordone, M.C. Motta, F. Picard, A. Robinson, U.S. Jhala, J. Apfeld, T. McDonagh, M. Lemieux, M. McBurney, A. Szilvasi, E.J. Easlon, S.J. Lin, L. Guarente, Sirt1 regulates insulin secretion by repressing UCP2 in pancreatic beta cells, PLoS Biol. 4(2) (2006):e31. Epub 2005 Dec 27.

[71] F. Picard, M. Kurtev, N. Chung, A. Topark-Ngarm, T. Senawong, R. Machado De Oliveira, M. Leid, M.W. McBurney, L. Guarente, Sirt1 promotes fat mobilization in white adipocytes by repressing PPAR-gamma, Nature 429 (6993) (2004) 771-776.

[72] L. Qiang, L. Wang, N. Kon, W. Zhao, S. Lee, Y. Zhang, M. Rosenbaum , Y. Zhao, W. Gu, S.R. Farmer, D. Accili, Brown remodeling of white adipose tissue by SirT1-dependent deacetylation of Pparγ, Cell 150 (3) (2012) 620-632.

[73] C. Xu , B. Bai, P. Fan, Y. Cai, B. Huang, I.K. Law, L. Liu, A. Xu, C. Tung, X. Li, F.M. Siu, C.M. Che, P.M. Vanhoutte, Y. Wang, Selective overexpression of human SIRT1 in adipose tissue enhances energy homeostasis and prevents the deterioration of insulin sensitivity with ageing in mice, Am J Transl Res. 5(4) (2013) 412-426.

[74] M.T. Rached, A. Kode, L. Xu, Y. Yoshikawa, J.H. Paik, R.A. Depinho, S. Kousteni, FoxO1 is a positive regulator of bone formation by favoring protein synthesis and resistance to oxidative stress in osteoblasts, Cell Metab 11 (2) (2010)147-160.

[75] J. Nakae,T. Kitamura, Y. Kitamura, W.H. 3rd. Biggs, K.C. Arden, D. Accili, The forkhead transcription factor Foxo1 regulates adipocyte differentiation, Dev Cell 4 (1) (2003) 119-129.

[76] I. Gerin, G.T. Bommer, M.E. Lidell, A. Cederberg, S. Enerback, O.A. Macdougald, On the role of FOX transcription factors in adipocyte differentiation and insulin-stimulated glucose uptake, J Biol Chem. 284 (16) (2009) 10755-1063.

[77] M.F. Siqueira, S. Flowers, R. Bhattacharya, D. Faibish, Y. Behl, D.N. Kotton, L. Gerstenfeld, E. Moran, D.T. Graves, FOXO1 modulates osteoblast differentiation, Bone 48 (5) (2011)1043-1051.

[78] H.N. Kim, L. Han, S. Iyer, R. de Cabo, H. Zhao, C.A. O'Brien, S.C. Manolagas, M. Almeida, Sirtuin1 Suppresses Osteoclastogenesis by Deacetylating FoxOs, Mol Endocrinol. 29 (10) (2015)1498-1509.

[79] C.J. Lynch, Z.H. Shah., S.J. Allison, S.U. Ahmed, J. Ford, L.J. Warnock, H. Li, M. Serrano, J. Milner, SIRT1 Undergoes Alternative Splicing in a Novel Auto-Regulatory Loop with p53, PLoS ONE 5 (10) (2010) e13502.

[80] S. Huhn, F. Beyer, R. Zhang, L. Lampe, J. Grothe, J. Kratzsch, A. Willenberg, J. Breitfeld, P. Kovacs, M. Stumvoll, R. Trampel, P.L. Bazin, A. Villringer, A.V. Witte, Effects of resveratrol on memory performance, hippocampus connectivity and microstructure in older adults - A randomized controlled trial, Neuroimage 174 (2018) 177-190.

[81] A. Hoseini, G. Namazi, A. Farrokhian, Z. Reiner, E. Aghadavod, F. Bahmani, Z. Asemi, The effects of resveratrol on metabolic status in patients with type 2 diabetes mellitus and coronary heart disease, Food Funct. 10 (9) (2019) 6042-6051.

[82] M. Akbari, O.R. Tamtaji, K.B. Lankarani, R. Tabrizi, E. Dadgostar, F. Kolahdooz, M. Jamilian, H. Mirzaei, Z. Asemi, The Effects of Resveratrol Supplementation on Endothelial Function and Blood Pressures Among Patients with Metabolic Syndrome and Related Disorders: A Systematic Review and Meta-Analysis of Randomized Controlled Trials, High Blood Press Cardiovasc Prev. 26 (4) (2019) 305-319.